 CMES, vol.78, no.3, pp.151-168, 2011

Topological Optimization of Anisotropic Heat Conducting Devices using Bezier-Smoothed Boundary Representation

C.T.M. Anflor[1] **and R.J. Marczak**[2]

Abstract: This paper aims to demonstrate the final result of an optimization process when a smooth technique is introduced between intermediary iterations of a topological optimization. In a topological optimization process is usual irregular boundary results as the final shape. This boundary irregularity occurs when the way of the material is removed is not very suitable. Avoiding an optimization post-processing procedure some techniques of smooth are implemented in the original optimization code. In order to attain a regular boundary a smoothness technique is employed, which is, Bezier curves. An algorithm was also developed to detect during the optimization process which curve of the intermediary topology must be smoothed. For the purpose of dealing with non-isotropic materials a linear coordinate transformation was implemented. Afterwards, some cases are compared and discussed.

Keywords: Shape optimization, boundary elements, topological derivative, Bezier, Orthotropic Materials.

1 Introduction

Classical topological optimization, based on the homogenization or the density approach [Bendsøe and Kikuchi (1988) ; Hassani and Hinton (1998)], often used for elasticity problems presents some drawbacks. One of these drawbacks refers to the final and intermediary topology from an optimization process, which results an appearance of sawtooth shape boundaries. This final shape irregularity frequently requires a post-processing. Final shapes obtained by sensitivity analysis using topological derivative [Novotny, Feijóo, Taroco and Padra, (2003)] also results in an irregular shape due to the way of the material was removed, independently of the optimization method. An irregularity in the boundary, such as sized rectangular cells, is not suitable because it causes a field concentration around sharp corners.

[1] UnB, Brasília, DF, Brazil.
[2] UFRGS, Porto Alegre, RS, Brazil

In order to overcome these defects also presented in a previous work [Marczak (2007)], a new methodology for topology optimization is implemented in the original code. The main idea of this work relies in smooth the boundary during the process optimization, where shape and topology optimization are simultaneously performed in the design process. A smoothness technique is implemented and after its final shapes is compared with those obtained from the classical optimization solution. Figure 1 illustrates a BEM mesh smoothed by Bezier interpolation.

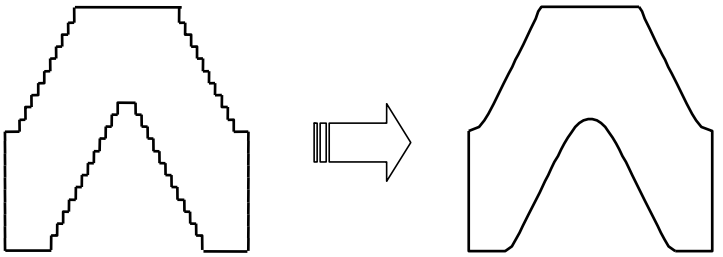

Figure 1: Example of boundary smoothing. (a) Original result. (b) Beziér-smoothed result

Attaining this objective, the concepts of a topological derivative (TD) and a section of smooth method are introduced and successfully combined with the classical shape optimization. A number of linear heat transfer examples are solved with the formulation proposed. The irregular boundaries from the final and intermediaries shapes are eliminated. Materials with non-isotropic behavior are also considerate. The results are compared to those available in the literature.

2 Numerical Methodology

BEM's code was developed in its direct version using the fundamental solution to isotropic materials. The linear coordinate transformation method [Poon, Tsou and Chang (1979) ; Poon (1979)] is introduced in this routine. This technique allows the solving of anisotropic heat transfer problems, avoiding changes in the BEM code and manipulations of the TD formulas. The governing differential equation for the heat conduction problem in a two-dimensional Cartesian coordinate system is given in its full form by:

$$k_{11}\frac{\partial^2 T}{\partial x^2}+2k_{12}\frac{\partial^2 T}{\partial x\partial y}+k_{22}\frac{\partial^2 T}{\partial y^2}=0 \tag{1}$$

Where , k_{11}, k_{12} and k_{22} are the thermal conductivity coefficients, while T represents the field temperature. The corresponding heat fluxes are expressed as:

$$\begin{aligned} q_x &= -k_{11}\frac{\partial T}{\partial x} - k_{12}\frac{\partial T}{\partial y} \\ q_y &= -k_{12}\frac{\partial T}{\partial x} - k_{22}\frac{\partial T}{\partial y} \end{aligned} \tag{2}$$

The initial geometry (x) established in an anisotropic medium is converted into an equivalent isotropic problem ($\hat{x}$) by using the coordinate transformation.

A special linear coordinate transformation is introduced to transform the partial differential equation into the Laplace equation as:

$$\begin{aligned} \hat{x} &= x + \alpha \cdot y \\ \hat{y} &= \beta \cdot y \end{aligned} \tag{3}$$

Where $\alpha = \frac{-k_{12}}{k_{22}}$, $\beta = \frac{k}{k_{22}}$, $k = \sqrt{k_{11}k_{22} - k_{12}^2}$.

Neumann boundary conditions must also be transformed according to the Eq. (4).

$$\begin{aligned} q_y &= -k\frac{\partial T}{\partial y} = q_{\hat{y}} \\ q_x &= \beta\, q_{\hat{x}} - \alpha\, q_{\hat{y}} \end{aligned} \tag{4}$$

To demonstrate the steps of the numerical implementation, a numerical methodology scheme will be presented in details. The optimization process is carried out in 7 steps (see Fig. 2):

Step 1 - Transform an orthotropic domain into an equivalent isotropic domain through the linear coordinate transformation expressed in Eq. (3). The heat flux is transformed by inverting Eq. (4).

Step 2 - Solve the problems by means of the BEM code developed to isotropic materials.

Step 3 - Apply the inverse of the mapping domain using equation to the geometry and to the heat flux.

Step 4 - The variables are evaluated on a suitable grid of interior points. The points with the lowest values of TD are selected.

Step 5 - Holes are created by “punching out” disks of material centered on the points previously selected.

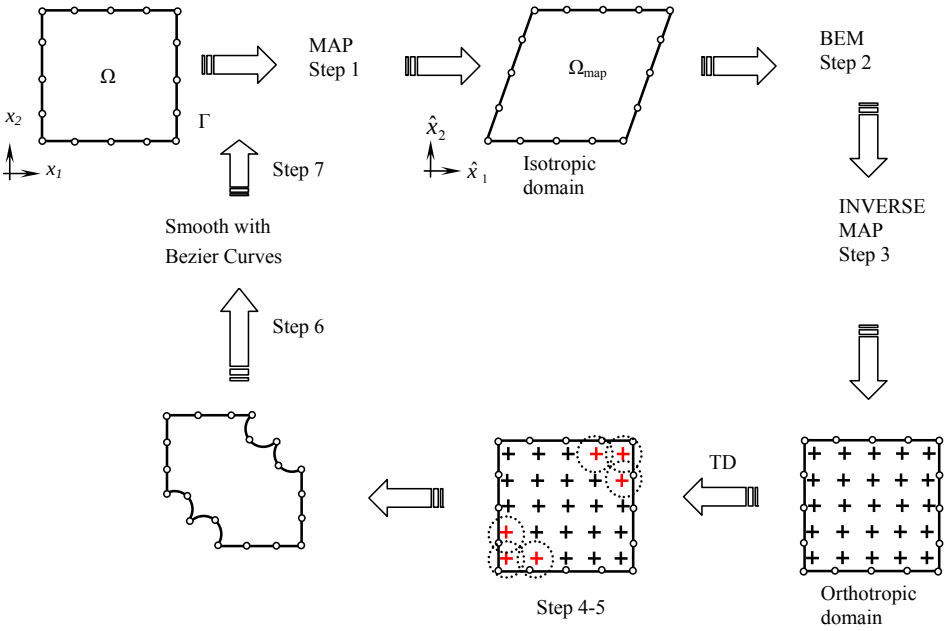

Figure 2: Numerical methodology scheme

Step 6 - Smooth process using Bezier Curves is introduced

Step 7 - Check stopping criteria, rebuild the mesh, return to step 1.

When the process is halted, a smooth final design topology of a non-isotropic material is expected.

In order to avoid some geometrical boundary irregularity due to the algorithm used to remove material, a smooth process is implemented at step 6. As a smoothness technique the Bezier Curve [Newman and Sproull (1982)] is chosen to treat the polylines of the intermediary geometry.

2.1 Topological Derivative

A topological derivative for Poisson Equation is applied in this work. A simple example of applicability consists in a case where a small hole of radius (ε) is open inside the domain. The concept of topological derivative consists in determining the sensitivity of a given function cost (ψ) when this small hole is increased or decreased. The local value of TD at a point ($\bar{\bar{x}}$) inside the domain for this case is

evaluated by:

$$\overset{*}{D}_T(\bar{\bar{x}}) = \lim_{\varepsilon \to 0} \frac{\psi(\Omega_\varepsilon) - \psi(\Omega)}{f(\varepsilon)}, \tag{5}$$

where $\psi(\Omega_\text{¸})$ and $\psi(\varepsilon)$ are the cost function evaluated for the original and the perturbed domain, respectively, and f is a problem dependent regularizing function. By Eq. 5 it is not possible to establish an isomorphism between domains with different topologies. This equation was modified [Feijóo, Novotny, Taroco and Padra (2003)] introducing a mathematical idea that the creation of a hole can be accomplished by single perturbing an existing one whose radius tends to zero. This allows the restatement of the problem in such a way that it is possible to establish a mapping between each other [Feijóo, Novotny, Taroco and Padra (2003)].

$$\overset{*}{D}_T(\bar{\bar{x}}) = \lim_{\varepsilon \to 0} \frac{\psi(\Omega_{\varepsilon+\delta\varepsilon}) - \psi(\Omega_\varepsilon)}{f(\Omega_{\varepsilon+\delta\varepsilon}) - f(\Omega_\varepsilon)}, \tag{6}$$

where $\delta\ddot{\text{A}}\varepsilon$ is a small perturbation on the holes's radius. In the case of linear heat transfer, the direct problem is stated as:

$$\text{Solve } \{u_\varepsilon | -k\Delta u_\varepsilon = b\} \text{ on } \Omega_\varepsilon \tag{7}$$

subjected to

$$\begin{cases} u_\varepsilon = \overline{u} & \text{on } \Gamma_D \\ k\frac{\partial u}{\partial n} = \overline{q} & \text{on } \Gamma_N \\ k\frac{\partial u_\varepsilon}{\partial n} = h_c\,(u_\varepsilon - u_\infty) & \text{on } \Gamma_R, \end{cases} \tag{8}$$

where

$$h(\alpha,\beta,\gamma) = \underbrace{\alpha\,(u_\varepsilon - \overline{u}^\varepsilon)}_{Dirichlet} + \underbrace{\beta\left(k\frac{\partial u_\varepsilon}{\partial n} + \overline{q}^\varepsilon\right)}_{Neumann} + \underbrace{\gamma\left(k\frac{\partial u_\varepsilon}{\partial n} + h_c^\varepsilon\,(u_\varepsilon - u_\infty^\varepsilon)\right)}_{Robin} = 0 \tag{9}$$

is a function which takes into account the type of boundary condition on the holes to be created (u_ε, $\frac{\partial u_\varepsilon}{\partial n} = q_\varepsilon$ are the temperature and flux on the hole boundary, while u_∞^ε and h_c^ε are the hole's internal convection parameters, respectively). After an intensive analytical work, [Feijóo, Novotny, Taroco and Padra (2003)] it was developed explicit expressions for TD for problems governed by (7). Table 1 presents the final expressions for topological derivative, considering the three classical cases of boundary conditions on the holes.

Table 1: Topological derivative for the various boundary conditions prescribed on the holes using the total potential energy as a cost function

Boundary condition on the hole	**Topological derivative**	**Evaluated at**
Neumann homogeneous boundary condition ($\alpha = 0$, β =1 , $\gamma = 0$)	$D_T(\overline{\overline{x}}) = k\nabla u \nabla u - bu$	$\overline{\overline{x}} \in \Omega \cup \Gamma$
Neumann non-homogeneous boundary condition ($\alpha = 0$, β =1 , $\gamma = 0$)	$D_T(\overline{\overline{x}}) = -q_\varepsilon u$	$\overline{\overline{x}} \in \Omega \cup \Gamma$
Robin boundary condition ($\alpha = 0$, β = 0, $\gamma = 1$)	$D_T(\overline{\overline{x}}) = h_c^\varepsilon (u_\varepsilon - u_\infty)$	$\overline{\overline{x}} \in \Omega \cup \Gamma$
Dirichlet boundary condition ($\alpha = 1$, $\beta = 0$, $\gamma = 0$)	$D_T(\overline{\overline{x}}) = -\frac{1}{2} k (u - \overline{u}_\varepsilon)$	$\overline{\overline{x}} \in \Omega$
Dirichlet boundary condition ($\alpha = 1$, $\beta = 0$, $\gamma = 0$)	$D_T(\overline{\overline{x}}) = k\nabla u \nabla u - b\overline{u}_\varepsilon$	$\overline{\overline{x}} \in \Gamma$

2.2 Bézier Curves

Generally in an optimizations process the final topology results in a non-smoothed geometry. It requires an employment of techniques of smoothness during the optimization process. In order to study the behavior of a final topology a technique where previously chosen to be implemented in the actual optimization code, as mentioned at step 6 (See |Fig. 2). The most popular techniques to deal with these irregular geometries are Bezier curves, Douglas-Peucker and B-Splines algorithm. This work uses the Bezier curves to smooth the topology resulted during the optimization process. The Bezier curve was pioneered used in a modeling of surface in automobile design by Renault (Newman and Sproull, 1982). Bezier defines the curve $P(u)$ in the terms of the location $n+1$ control points p_i.

$$P(u) = \sum_{i=0}^{n} p_i B_{i,n}(u) \tag{10}$$

where $B_{i,n}(u)$ is a blending function or polynomials of Bernstein

$$B_{i,n}(u) = C(n,i)\, u^i (1-u)^{n-i} \tag{11}$$

and $C(n,i) = \frac{n!}{i!(n-i)!}$ is the binomial coefficients.

Here, Eq. 10 is a vector and could be expressed by writing equations for the x and

y parametric functions separately:

$$x(u) = \sum_{i=0}^{n} x_i B_{i,n}(u)$$
$$y(u) = \sum_{i=0}^{n} y_i B_{i,n}(u) \tag{12}$$

x_i and y_i are the coordinates of the control points of the curve, always n+1 points. The union of this points form the vertices of the control polygon of the Bezier curve. These points are responsible to control the shape of the curve, with the parameter u varying between 0 to 1. Further details can be found in Harrington (1983). As exposed until here the techniques of smoothness curves are well established in the literature and there is no problem in apply them. But in an optimization problem the effort relies in identifying which portions of the intermediary topology must be smoothed. There are some parts of the topology that can not be smoothed, such as, the portion with prescribed boundary conditions or the portion which is a straight line. In order to overcoming this problem a routine is developed in the present work to identify during an iterative optimization process which curves must be or not smoothened. This routine was introduced inside the optimization algorithm as step 6, after the step of removal material (see Fig.2). Figure 3 depicts the scheme of identification and smoothness of curves resulted during the optimization process. This is a subroutine implemented between step 5 and 7 of the original code as illustrated in Fig.2.

3 Numerical Results

This section presents some examples that demonstrate the application of the proposed method. The results obtained for the first one are compared to those obtained by Park (1995) for isotropic materials. The second example differs from the first one only in the boundary conditions, which prescribed convection in the cavities. The third and fourth examples consist in a square domain under high and low temperature boundary conditions where the constitutive properties were varied to result in all possible behaviors: isotropic, orthotropic and anisotropic. The history of material removal is analyzed and illustrated for each case. The iterative process was halted when a given amount of material was removed from the original domain, regardless of the type of material medium. This criterion provided a basis to compare the topologies generated for isotropic, orthotropic and anisotropic media under the same initial geometry and boundary conditions. In all cases the total potential energy was used as the cost function. A regularly-spaced grid of internal points was generated automatically, taking into account the radius of the holes created during

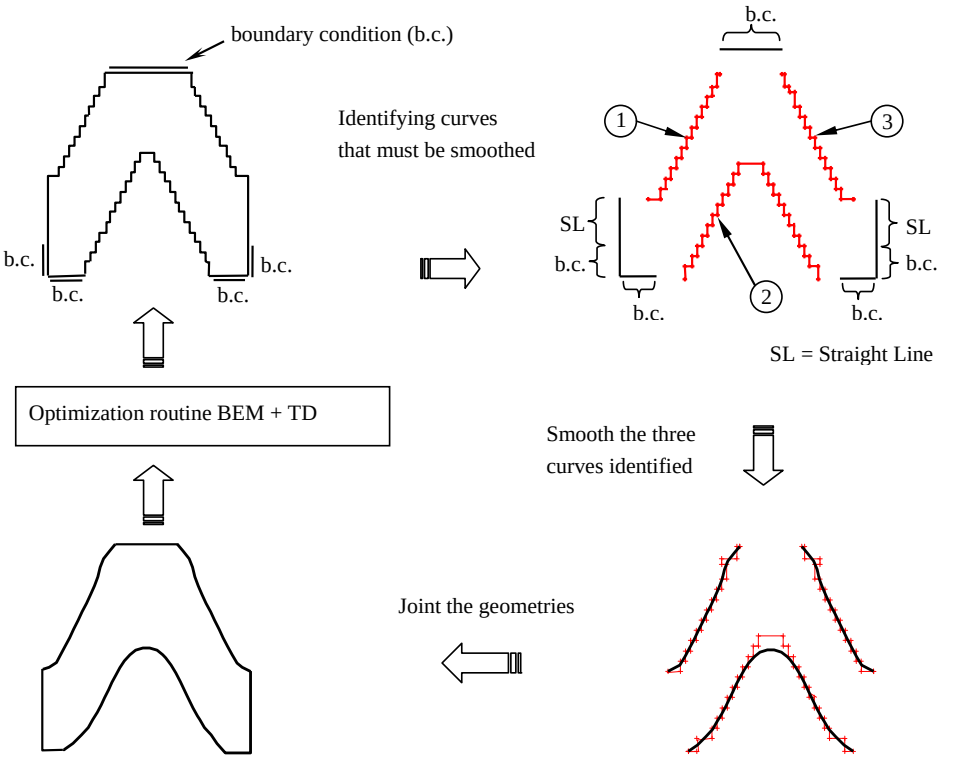

Figure 3: Scheme of identification and smoothness – Step 6

each iteration. The radius was obtained as a fraction of a reference dimension of the domain ($r = \omega\ l_{ref}$). In all cases l_{ref} =min(height,width) was adopted. The objective in all cases was to minimize the material area. The current area of the domain (A_f) was checked at the end of each iteration until a reference value was achieved ($A_f = \phi\ A_0$, where A_0 represents the initial area and ϕ a defined percentage of material to be removed). After that, the intermediary topology was smoothed by using Bezier function. Linear discontinuous boundary elements integrated with 4 Gauss points were used in all cases.

3.1 Heat conductor with Neumann boundary conditions on the cavities

A rectangular 20×30 units domain subjected to prescribed temperature ($T_1 = 393K$) on its left edge and convection boundary conditions ($T_0 = 298K$ and $h_0 = 5.677$ W/m^2K) on the remaining ones is to be optimized (Fig.4). Here, the problem is revisited using only isotropic material properties. The isotropic material used is

Aluminum (k = 236 W/mK). For this case, Neumann boundary conditions were prescribed on the cavities open during the optimization process.

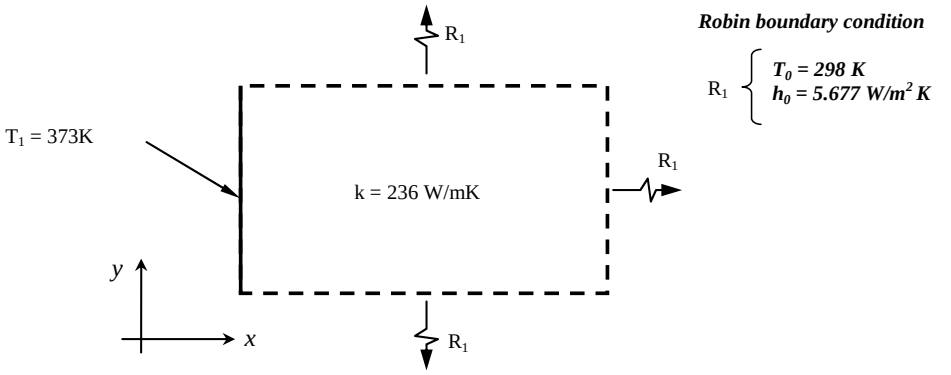

Figure 4: Initial design domain

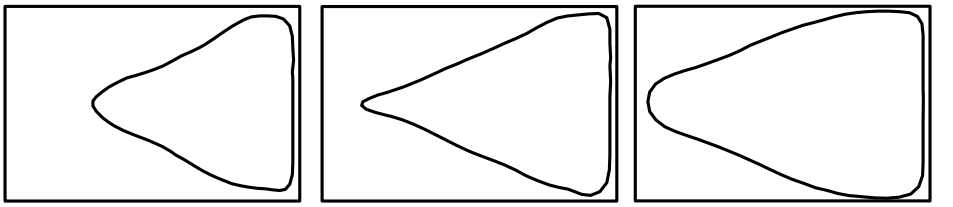

Figure 5: Evolution history for isotropic media

Figure 5 shows the evolution history obtained until the final area reached 30% of the original value. The final and intermediary topology results in a smooth appearance shape. It is important to note that the appearance of saw-tooth shape on boundaries was avoided, discarding a post-processing in a manufacturing process.

The mean flux on the left edge side of the plate is chosen to take into account the behavior as the process evolves. The values of the mean flux obtained during the process optimization with Bezier are recorded and compared with the result obtained with the original code without smoothness technique. These results are depicted in Fig. 6 where is possible to see the evolutive iteration $\times$ mean flux. Also, in the same figure the smoothed intermediary topology is depicted for some iterations.

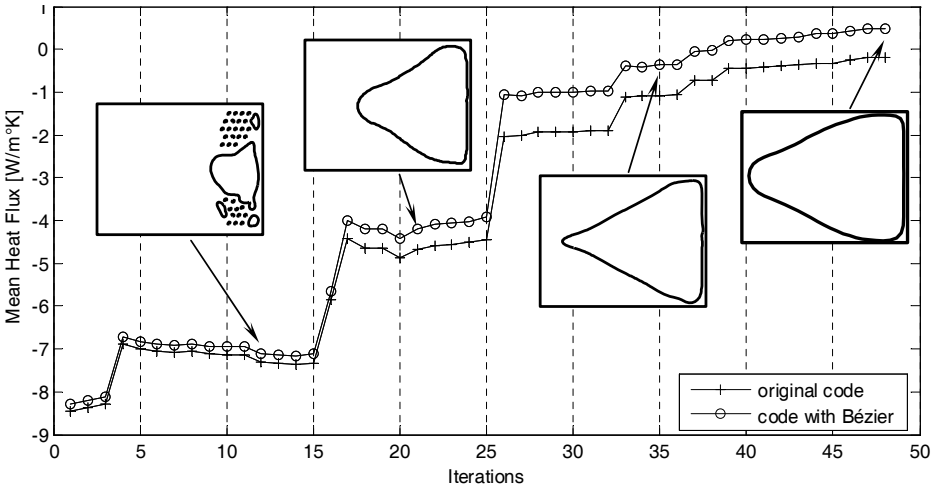

Figure 6: Optimization history of mean heat flux vs. iteration

In the orthotropic case, the thermal conductivities were imposed as $k_y/k_x = 2$. Figure 7 presents the evolution history obtained until the same volume ratio of the isotropic case was reached. Clearly, the resulting geometry of the internal cavity has a more pronounced curvature, so as to facilitate the heat transfer flux in the y direction.

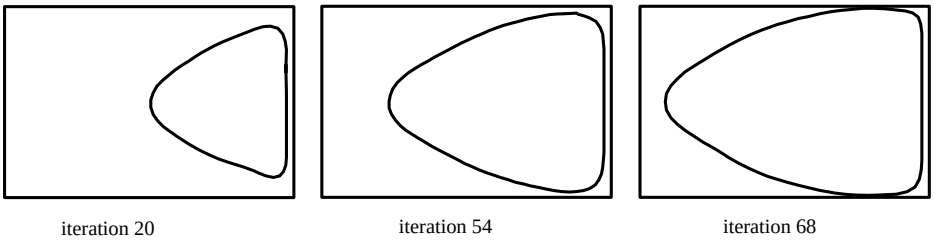

Figure 7: Evolution history for orthotropic media

Park (1995) solved this problem by using homogenization techniques and the FEM. Figure 8 compares the results obtained by Park (1995) with the ones obtained with the present method. In all cases, the final geometry is satisfactorily leading to a high-conductivity layout, and both isotropic results match.

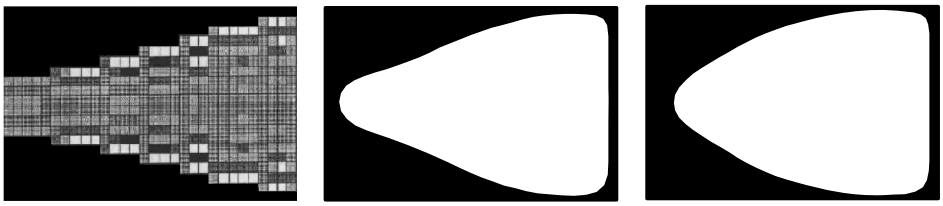

(a) (b) (c)

Figure 8: Final topologies: (a) FEM+homogeneization (Park, 1995) – $k_x/k_y = 1$; (b) Present work, BEM+ *TD* – $k_x/k_y = 1$; (c) Present work, BEM+*TD* – $k_y/k_x = 2$

3.2 Heat conductor with Robin boundary conditions on the cavities

This case is very similar to the previous one, except for the fact that the convection boundary condition was imposed on the cavities. This is an isotropic case optimized to a volume constraint of 65% of the original design domain. The evolution of the optimization process is depicted in Fig. 9. It is important to point out that the final geometry converged to the shape of an optimal fin.

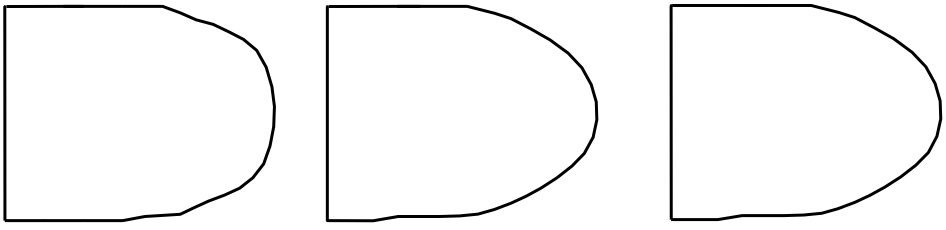

iteration 17 iteration 26 iteration 28

Figure 9: Evolution history under Robin boundary conditions

3.3 Inverted V heat conductor

This example consisted in a square domain with high temperature (373 K) applied to its lower corners, while a low temperature (273 K) was applied at the mid top edge. The remaining boundaries were insulated. The cavities were created with $r = 0.04 l_{ref}$ and the processwas halted when $A_f = 0.6\, A_0$ was attained. For the purpose of illustrating and comparing the final topologies obtained, three variations of the present example are studied as:

Case A: $k_{xx} = 1$; $k_{yy} = 1$

Case B: $k_{xx} = 2$; $k_{yy} = 1$

Case C: $k_{xx} = 3$; $k_{yy} = 1$

Figure 10 shows the results for the isotropic case (case A) which is used to compare the final design with those of the orthotropic cases (cases B and C). Figures 11 and 12 present the optimization evolution for the orthotropic cases and their final topologies when the stop criteria were achieved. From this it is possible to compare the three cases. There are visible differences in the evolution of material removal for each case. Therefore, the final designs are slightly different in this case.

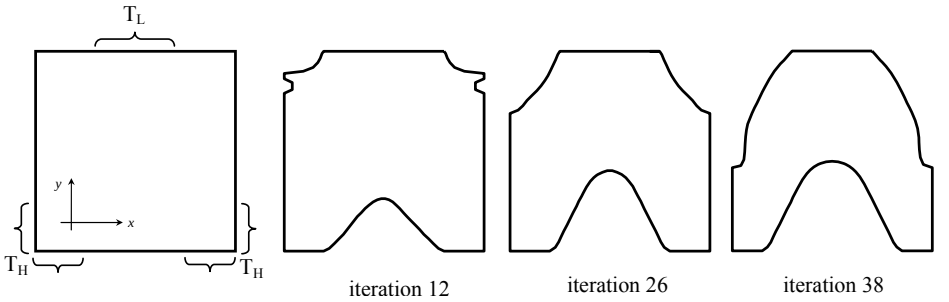

Figure 10: Evolution history for isotropic material – Case A

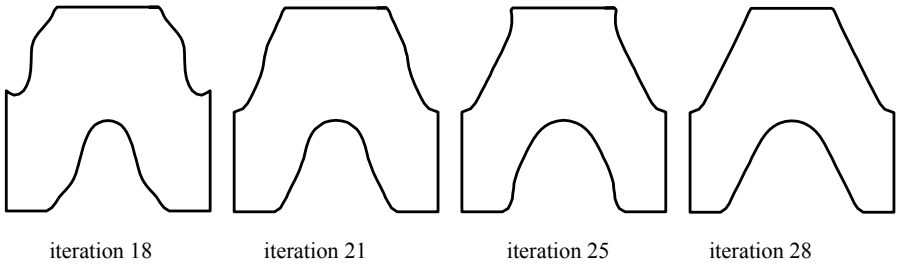

Figure 11: Evolution history for orthotropic material – Case B

Figure 13 presents the evolution of the material removal for all cases. It was found that highly orthotropic cases result in higher values of the topological sensitivity, in comparison to the isotropic solution. Consequently, a larger material removal rate is expected for orthotropic problems, in general, but this is an assertion that highly depends on the nature of the problem.

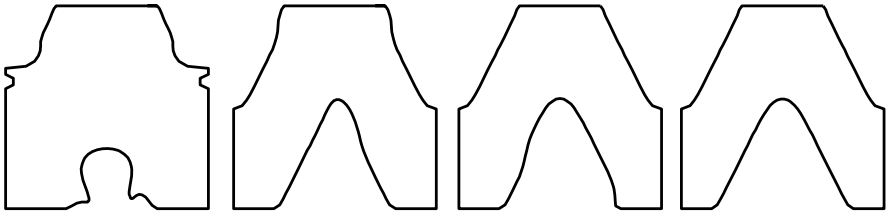

Figure 12: Evolution history for orthotropic material – Case C

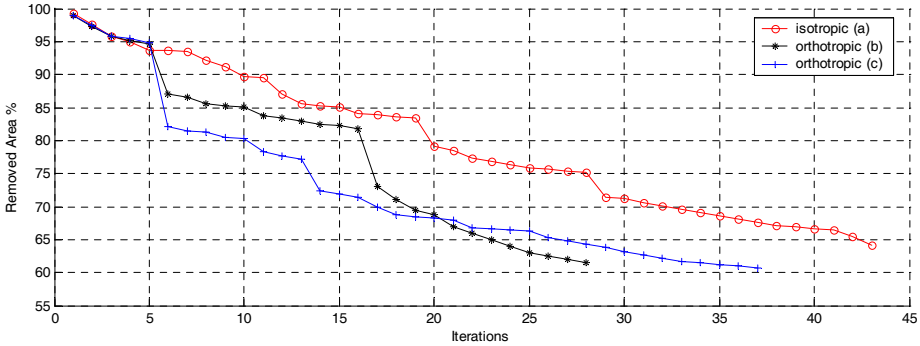

Figure 13: Material removal history for the Inverted V heat conductor

3.4 Cross Heat Conductor

This example refers to a square domain subjected to low and high temperature boundary conditions on the middle of opposite sides. The problem is depicted in Fig.14, where T_H is the high temperature (373 K) and T_L is the low temperature (273 K). The remaining boundaries are insulated. All possible cases will be studied: isotropic, orthotropic and anisotropic materials and they are to be optimized until $A_f \approx 0.4\, A_0$ is achieved.

Initially, an isotropic case was analyzed with $k_{11} = k_{22} = 1$. Symmetry was not used to provide a direct comparison to the subsequent anisotropic cases (which cannot use symmetry). Figure 14 also shows the evolution of material removal for $r = 0.02 l_{ref}$. It is important to observe that the algorithm delivered fairly symmetric solutions throughout the process. The condition $A_f \approx 0.4 \bullet A_0$ was achieved after 34 iterations. The second case represents a highly orthotropic material, with the conductivities set to $k_{xx} = 5$ and $k_{yy} = 1$ (see Fig.15). As expected, material is selectively removed so that the heat flux along the x direction is increased. The

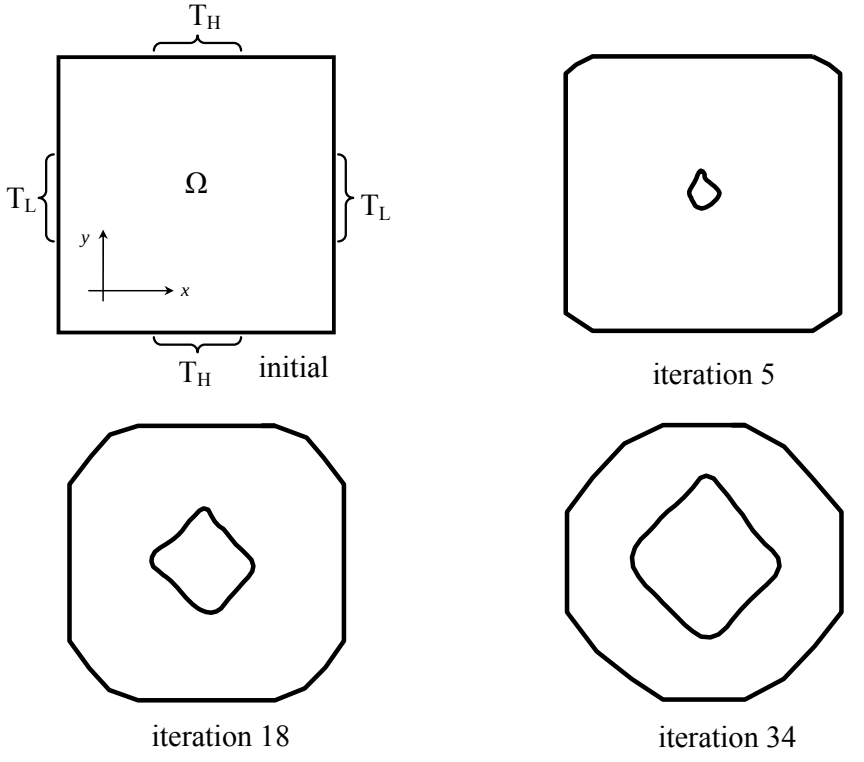

Figure 14: Evolution history for isotropic case ($k_{xx} = k_{yy} = 1$).

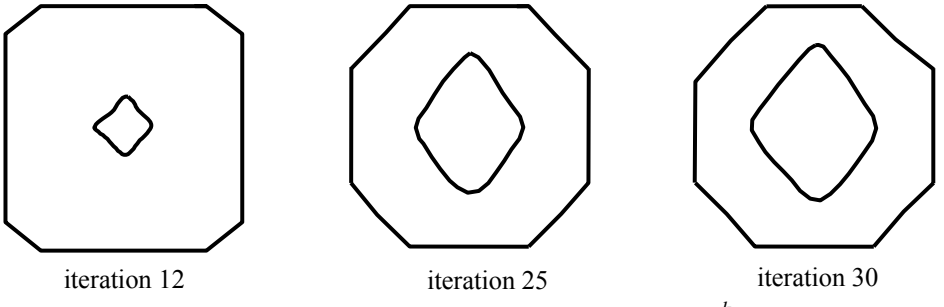

Figure 15: Evolution history for orthotropic case ($\frac{k_{xx}}{k_{yy}} = 5$)

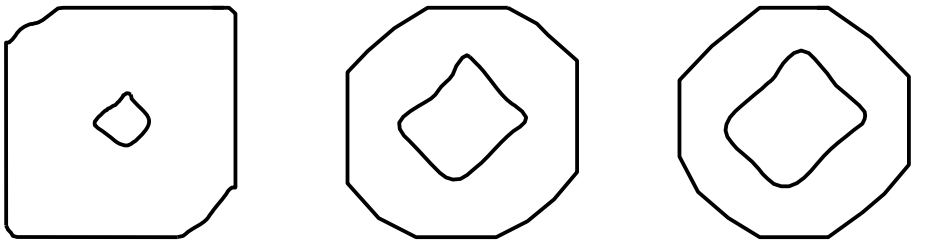

iteration 12 iteration 34 iteration 41

Figure 16: Evolution history for anisotropic case ($k_{xx} = k_{yy} = 1\ ;\ k_{xy} = 0.5$)

stop criterion $A_f \approx 0.4\, A_0$ was achieved after 30 iterations.

The third case considers an anisotropic material with $k_{xx} = 1$, $k_{yy} = 1$ and $k_{xy} = 0.5$. The evolution history is presented in Fig.16, showing that the initial symmetry is lost after the first iterations, as expected. Contrary to the previous cases, the internal cavity resulted in a rhombic shape since the Cartesian axes are not parallel to the main axes of the constitutive matrix.

Figure 17 shows the percentage of material removed as a function of the number iterations for each case studied in the cross heat conductor. All cases were stopped when about 40% of material was removed. These cases were analyzed without the aid of symmetry, for comparison purposes. Obviously, anisotropic cases cannot use symmetry in general, but in many practical situations it is possible (or even expected) to align the axes of the component with the principal directions of the constitutive matrix. In such cases, smoother designs can be obtained. In order to provide a further benchmark, the cross heat conductor example was re-analyzed for the isotropic and orthotropic cases using only one quadrant of the original geometry.

Figure 18 shows the final topologies obtained for both cases while Fig.19 depicts the same topology after the smoothness process. The material was removed initially with $r = 0.04\ l_{ref}$ and then $r = 0.02\ l_{ref}$. for the remaining iterations. This simple expenditure helps generate smoother boundaries in the final design.

4 Conclusions

Complex shapes with irregularities on their boundaries frequently result after a topology optimization. In this paper a smoothness technique was employed in order to avoid a new task of post-processing over the resulting topology. This procedure allowed attaining more realistic geometries when the optimization was halted. In

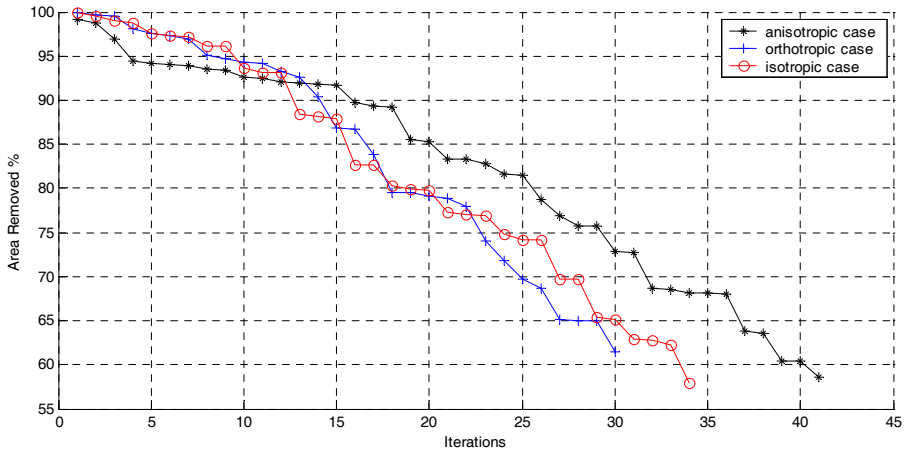

Figure 17: Material removal history for the cross heat conductor

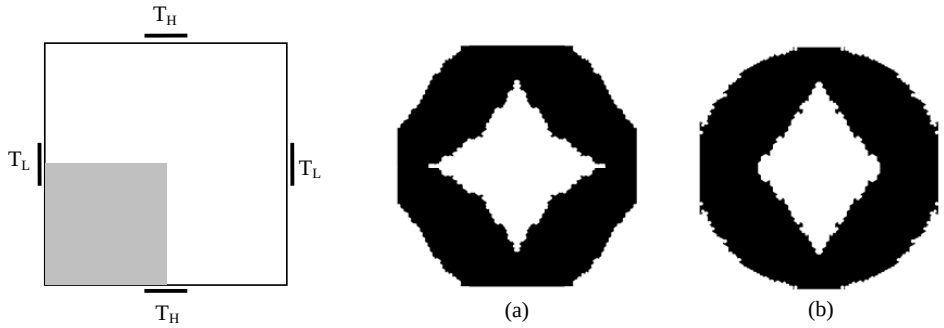

Figure 18: Final topologies for: (a) isotropic and (b) orthotropic examples

order to deal with those resulting irregular boundaries a smoothness using Bezier curve was used. This technique permits to result in a suitable geometry which provides, for example, a manufacturing of the final design without the designer interference. A linear coordinate transformation method was also implemented providing to extend the analysis to non isotropic materials behavior. This allowed the use of TD, since this formulation was deduced only for isotropic materials. The linear heat transfer problems were solved showing the feasibility of the procedure proposed and agreement with other solutions.

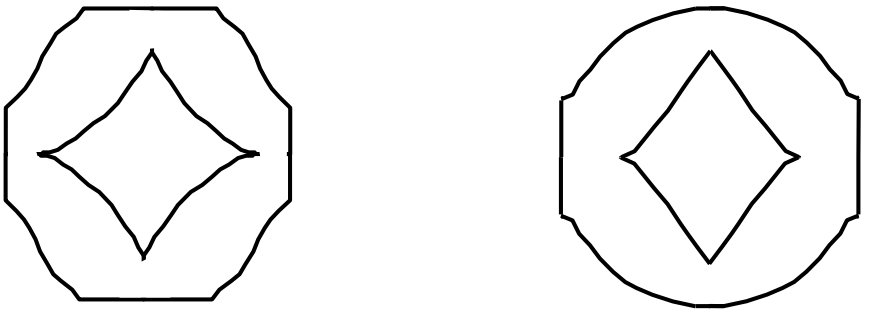

(a) (b)

Figure 19: Bezier final topologies for: (a) isotropic and (b) orthotropic examples

References

Bendsøe, M. P.; Kikuchi N. (1988): Generating optimal topologies in structural design using a homogenization method. *Comput. Methods Appl. Mech. Engrg*, vol. 71, pp. 197-224.

Feijóo, R.; Novotny,A.; Taroco, E.; Padra, C. (2003): The topological derivative for the poisson's problem. *Mathematical Models and Methods in Applied Sciences*, vol.13, pp. 1825-1844.

Harrington, S. (1983): *Computer Graphics: A programming approach*, McGraw-Hill.

Hassani, B.; Hinton, E. (1998): A review of homogenization and topology optimization III - topology optimization using optimality criteria. *Computers and Structures*, vol. 69, pp. 739-756.

Marczak R.J.; (2007) Topology Optimization and Boundary Elements – A Preliminary Implementation for Linear Heat Transfer. *Engineering Analysis with Boundary Elements*, vol. 31, pp. 793-802.

Newman, W.M.; Sproull R.F. (1982): *Principles of interactive computer graphics*. McGraw-Hill, New York.

Novotny, A.; Feijóo, R.; Taroco, E.; Padra, C. (2003): Topological-shape sensitivity analysis. *Comput. Methods Appl. Mech. Engrg.*, vol. 192, pp. 803–829.

Park Y.K. (1995): *Extensions of optimal layout design using the homogenization method*, Ph.D. Thesis, The University of Michigan, East Lansing Michigan.

Poon K.C.; Tsou R.C.H., Chang Y.P. (1979): Solution of anisotropic problems of first class by coordinate-transformation. *J. Heat Transfer*, vol. 101, pp. 340–345.

Poon K.C. (1979): Transformation of heat conduction problems in layered composites from anisotropic to orthotropic. *Lett. Heat Mass Transfer*, vol. 6, pp. 503–511.